

PHYSICAL REVIEW E

STATISTICAL PHYSICS, PLASMAS, FLUIDS, AND RELATED INTERDISCIPLINARY TOPICS

THIRD SERIES, VOLUME 51, NUMBER 6 PART A

JUNE 1995

RAPID COMMUNICATIONS

The Rapid Communications section is intended for the accelerated publication of important new results. Since manuscripts submitted to this section are given priority treatment both in the editorial office and in production, authors should explain in their submittal letter why the work justifies this special handling. A Rapid Communication should be no longer than 4 printed pages and must be accompanied by an abstract. Page proofs are sent to authors.

Percolation and the pore geometry of crustal rocks

Mark A. Knackstedt

*Department of Applied Mathematics, Research School of Physical Sciences and Engineering, Australian National University,
Canberra, Australian Capital Territory 0200, Australia*

Stephen F. Cox

*Petrophysics Group, Research School of Earth Sciences, Australian National University,
Canberra, Australian Capital Territory 0200, Australia*

(Received 19 December 1994)

Properties of isostatically compacted aggregates provide insight into the transport properties and the pore-space morphology of sedimentary rocks at depth in the Earth's crust. Here we provide evidence that percolation provides a natural description of the evolution of pore-space topology in compacted aggregates. Topological and transport properties of isostatically compacted aggregates measured by Zhang *et al.* [J. Geophys. Res. **99**, 15 741 (1994)] are modeled as a percolation process. Critical exponents associated with both topological quantities and transport properties are measured near the percolation transition and are consistent with the ordinary percolation universality class. We discuss how the use of percolation concepts (e.g., the backbone) facilitates the improved modeling of fluid migration in the crust.

PACS number(s): 05.40.+j, 72.15.Cz

Fluid transport in the crust plays a vital role in geothermal energy recovery, toxic waste isolation, the deposition of ores, and hydrocarbon accumulation [1]. Migrating crustal fluids are also implicated in controlling the mechanics of earthquake faulting [2]. The relationship between fluid transport and pore morphology under crustal conditions (e.g., during compaction, decementation, and deformation) is of fundamental importance to understanding fluid transport through rocks in sedimentary basins and active fault zones. Despite its significance, the understanding of fluid transport in the Earth's crust is poorly developed and remains an active research field [1].

Many studies have attempted to characterize the dependences of permeability and porosity on the stresses, pore pressure, lithology, and rock fabric [3–6]. Of fundamental interest is how the compaction mechanism influences the relation between porosity and transport properties (e.g., permeability and conductivity) [7–9]. In diagenetic and tectonic processes, significant permeability change is induced by

compaction processes involving cementation, intragranular plastic deformation, and solution precipitation. The temporal evolution of permeability in such cases is expected to be very complex, since the evolution of the pore space is controlled by the kinetics of the chemical process, diffusive mass transfer and crystal plasticity as well as fluid transport. Nevertheless, recent laboratory experiments under controlled conditions suggest that in physical compaction processes, transport properties and porosity can be related in a simple manner. In a seminal study Bernabe and co-workers [5,10] used isostatic hot pressing to mimic the compaction of rock under crustal conditions. The data showed an accelerated reduction in permeability as the calcite aggregates were compacted below 10% porosity. At porosities less than 4% the permeability vanished, implying a complete loss of connectivity in the pore space. More recently, Zhang *et al.* [11] conducted careful *in situ* measurements of permeability during hot pressing of calcite aggregates. In this paper we show the evolution of the pore geometry in the isostatic hot-

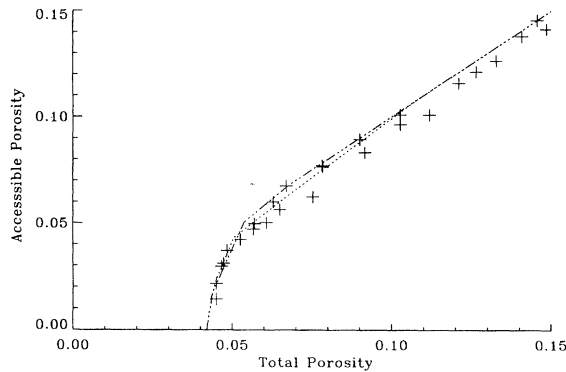


FIG. 1. Relationship between total porosity and connected porosity as determined in the experiments of Zhang *et al.* [11] (+). The two curves give the prediction of percolation: $Z=6$ (---); $Z=14$ (···).

pressing experiments of Zhang *et al.* is quantitatively described as a percolation process. The topological properties of the pore space of the rock are directly mapped onto the percolation model. Topological quantities associated with the percolation model are evaluated across the full range of the percolation probability. Critical exponents associated with both topological properties (the percolation probability) and transport properties (the permeability) are evaluated near the percolation transition and are in the ordinary percolation universality class. We discuss how the use of percolation concepts will facilitate the improved modeling of fluid transport in the crust.

We start with a description of the measurements of porosity and permeability evolution during hot pressing of calcite aggregates obtained by Zhang *et al.* [11]. The hot isostatic pressing of cold-pressed calcite aggregates was conducted in an internally heated argon-gas-medium, high pressure apparatus [12]. Permeability was measured *in situ* during hot pressing using techniques described by Fischer and Paterson [13]. Pore pressure during the experiments ranged from 130 MPa to 250 MPa while confining pressure ranged from 200 MPa to 300 MPa. During each run effective pressure (which equals confining pressure – pore pressure) was held constant. Time dependent porosity and permeability reductions were measured under isothermal conditions. The measurements of total porosity vs connected porosity and total porosity vs permeability are summarized in Figs. 1 and 2. It is evident from the connected porosity data that the closing off of porosity is significant at porosities less than 0.07. The permeability data show a deviation from a cubic law relating total porosity and permeability at total porosities less than 0.12, with a marked decrease evident for porosities less than 0.07.

We analyze the pore-space evolution of the hot-pressed aggregates in the context of a percolative phenomenon [14,15]. As shown in Fig. 1 Zhang *et al.* [11] directly measure the connected porosity during hot-isostatic-pressing of the calcite aggregates. It is evident that the sample becomes totally disconnected at porosities lower than 0.04. We identify p_c with the experimentally well-defined value of the critical porosity ($\phi_c=0.04$) below which the pore space becomes totally disconnected and fluid transport ceases. We assume the overall loss of connectivity as one approaches

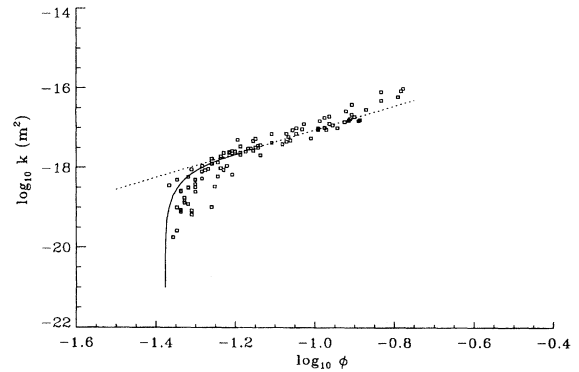


FIG. 2. Dependence of the permeability on total porosity as determined in the experiments of Zhang *et al.* [11] (\square). The relationship $k \propto \phi^3$ is given by the curve (···). Near ϕ_c the fit of $k(\phi) \propto (\phi - \phi_c)^2$ is shown by the solid line.

p_c is linearly related to the porosity reduction [16]. The aggregate at a significantly larger porosity can be described by a random network with an average coordination number (Z) on which cracks and pores are randomly distributed [17]. The experimentally measurable coordination number can be matched to the pore structure of the uncompressed aggregate. However, as we shall show, this choice of Z is not critical to the quantitative prediction of the connected porosity data. We consider percolation on the two regular three-dimensional networks: the simple-cubic lattice (sc) and the body-centered-cubic lattice (bcc) which exhibit coordination numbers of $Z=6$ and $Z=14$, respectively. The occupancy fraction of the lattice percolation model across the range of experimental porosity is determined by matching p_c of the lattice model to the experimental $\phi_c=0.04$. For the sc lattice $p_c(Z=6)=0.25$ and for the bcc lattice $p_c(Z=14)=0.09$ [15,18]. The choice of Z therefore determines the value of the experimental porosity matching $p=1$ in the model $\phi(p=1)$ [19].

We now consider the properties of the calcite aggregates quantitatively in the context of percolation. One important topological property of percolation networks is the accessible fraction $X^a(\phi)$ (the fraction of occupied bonds belonging to the infinite cluster). This can be evaluated for various lattices of different coordination number from simulation [14]. We perform computer simulations of percolation on both the sc and the bcc networks to evaluate $X^a(p)$. $X^a(\phi)$ is defined by the mapping from ϕ to p . We show in Fig. 1 a plot of $X^a(\phi)$ versus ϕ for bond percolation on the two three-dimensional lattices. This illustrates that the choice of Z , which affects the value of $\phi(p=1)$, does not substantially affect the property $X^a(\phi)$. The experimental data shown in Fig. 1 are in excellent agreement with the ordinary percolation behavior. It is clear that the evolution of the pore-space topology is described by the ordinary percolation model.

The numerical value of every percolation quantity depends on the microscopic details of the system. But near the percolation threshold most percolation quantities obey scaling laws that are largely insensitive to the network structure and its microscopic details. In ordinary percolation the exponent β_p characterizing the topological quantity $X^a(\phi)$ is completely universal, i.e., independent of the microscopic

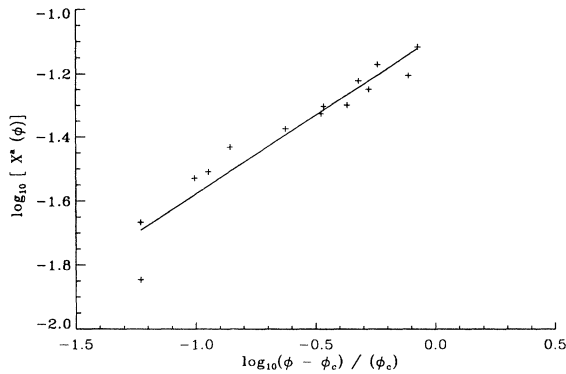


FIG. 3. Dependence of accessible porosity $X^a(\phi)$ on $\phi - \phi_c$. Best fit to the experimental data gives $X^a(\phi) \propto (\phi - \phi_c)^{0.45 \pm 0.1}$.

details of the system and depends only on the dimensionality of the system. In three dimensions percolation theory gives $X^a(p) \sim (\phi - \phi_c)^{\beta_p}$ with $\beta_p = 0.41$. We show in Fig. 3 the experimental behavior of $X^a(\phi)$ versus $(\phi - \phi_c)$ from which we obtain $\beta_p = 0.45 \pm 0.1$ consistent with the ordinary percolation result.

The percolation network may represent the pore space of a porous medium in which a fraction of the pores are open to flow. Thus a hydrodynamic permeability can also be defined. These transport properties are known to obey scaling laws near the percolation threshold and the transport exponents are largely universal. Near ϕ_c the permeability of a percolating network obeys the scaling law, $k(\phi) \propto (\phi - \phi_c)^e$ where $e = 2.0$ is the currently accepted value. Figure 4 illustrates the experimental porosity and permeability data from which $e = 1.9 \pm 0.2$ is obtained. Figure 2 shows a fit of the experimental data to a scaling law of the form $k(\phi) \propto (\phi - \phi_c)^2$. Clearly the evolution of the pore morphology during isostatic compression is quantitatively consistent with an ordinary percolation process [20].

The present results indicate that knowledge about percolation networks can be used for modeling the pore geometry of crustal rocks. An example of how the quantitative connection between pore geometry of crustal rocks and percolation will lend important insight into the fluid transport processes in crustal rocks is in determining the actual fluid-carrying portion (or backbone) of the pore space of crustal rocks. The topological exponent describing the *backbone* fraction of oc-

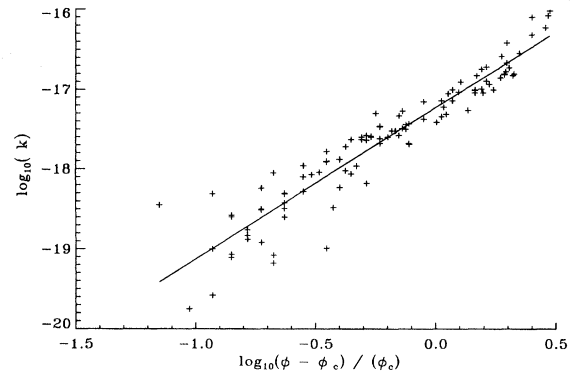


FIG. 4. Dependence of permeability k on $\phi - \phi_c$. Best fit to the experimental data gives $k(\phi) \propto (\phi - \phi_c)^{1.9 \pm 0.2}$.

cupied bonds near p_c is very different from the exponent describing the accessible fraction [15]. Knowledge of the backbone or fluid carrying porosity will aid in the understanding of fluid transport in crustal rock at low porosities.

The interpretation of densification of crustal rocks as percolationlike is not new (e.g., Bernabe [10] and Zhang *et al.* [11] observed that tubular pores along grain edges had been pinched off and attributed the dramatic decrease in permeability to connectivity loss in the pore space). However, in our work the pore properties have been mapped directly onto the percolation model and the percolation exponents evaluated experimentally.

The results suggest that percolation theory has application to the understanding of relationships between porosity, pore structure, and permeability in hydrocarbon reservoir and trap rocks in sedimentary basins. Even though changes in fluid transport properties involve intergranular chemical cementation and decementation processes, relationships between porosity and permeability in sandstone [8] exhibit qualitatively similar trends to those associated with purely mechanical compaction processes modeled in this study. For example, in the case of Fountainbleau sandstone a percolationlike threshold occurs at porosities of several percent [7,8].

The authors thank Shuqing Zhang for providing the experimental data upon which this analysis is based. M.A.K. and S.F.C. acknowledge the support of the Australian Research Council.

- [1] T. Torgersen, *Geophys. Res. Lett.* **18**, 917 (1991).
- [2] R. Sibson, *Tectonophysics* **211**, 283 (1992).
- [3] W. Brace, J. Walsh, and W. Frangos, *J. Geophys. Res.* **73**, 2225 (1968).
- [4] M. Zoback and J. Byerlee, *Am. Assoc. Pet. Geol. Bull.* **59**, 154 (1975).
- [5] Y. Bernabe, W. Brace, and B. Evans, *Mech. Mater.* **1**, 173 (1982).
- [6] C. David, T. F. Wong, and J. Zhang, *Pure Appl. Geophys.* (to be published).
- [7] P. Doyen, *J. Geophys. Res.* **93**, 7729 (1988).
- [8] J. Bourbie and B. Zinszner, *J. Geophys. Res.* **90**, 11 524 (1985).
- [9] W. Zhu, C. David, and T. Wong, *J. Geophys. Res.* (to be published).
- [10] Y. Bernabe, *Mech. Mater.* **5**, 235 (1986).
- [11] S. Zhang, M. Paterson, and S. Cox, *J. Geophys. Res.* **99**, 15 741 (1994).
- [12] M. Paterson, *Int. J. Rock Mech. Min. Sci.* **7**, 517 (1970).
- [13] G. Fischer and M. Paterson, in *Fault Mechanics and Transport Properties of Rocks*, edited by B. Evans and T. Wong (Academic, New York, 1993).

- [14] D. Stauffer and A. Aharony, *Introduction to Percolation Theory*, 2nd ed. (Taylor and Francis, London, 1992).
- [15] M. Sahimi, *Applications of Percolation Theory*, 1st ed. (Taylor and Francis, London, 1994).
- [16] The approximation that loss of connectivity is linearly related to porosity reduction is based on experimental measurements of sandstone and hot-pressed calcite aggregates at low porosities. Pore-space connectivity is clearly reduced during porosity reduction [11,21]. From the measurement of the pore size distribution [7,22] the hydraulic radius is approximately the same across a range of the porosity near the pore closure (percolation) threshold. While pore shrinkage may occur, the overall densification near p_c is dominated by pore closure.
- [17] A topologically disordered network would give a more realistic mapping of the rock pore space. We choose regular networks since, as shown by Jerauld and co-workers [18,23], percolation properties of topologically disordered systems are essentially identical to regular networks with the same connectivity.
- [18] G. Jerauld, L. Scriven, and H. Davis, *J. Phys. C* **17**, 3429 (1984).
- [19] The value of the percolation threshold depends primarily on the average coordination number. In the model the porosity at “total” connectivity is given for any Z by $\phi_Z(p=1) = \phi/p_c(Z)$.
- [20] Transport in percolating continua can be described by different exponents from percolation in discrete networks. Our results are inconsistent with the continuum percolation model which gives an exponent for permeability $e=4.4$ [24]. Moreover, visual images of hot-pressed calcite materials at low porosities [21] show the pore space is primarily made up of tubular pores aligned along three grain edges. The pore structure therefore mimics a porous network.
- [21] D. L. Olgaard and J. D. FitzGerald, *Contrib. Mineral. Pet.* **115**, 138 (1993).
- [22] J. Fredrich, K. Greaves, and J. Martin, *Int. J. Rock Mech. Min. Sci.* **30**, 691 (1993).
- [23] G. Jerauld, Ph.D. thesis, University of Minnesota, 1985 (unpublished).
- [24] S. Feng, B. Halperin, and P. Sen, *Phys. Rev. B* **35**, 197 (1987).